

# Encoding of Vibrissal Active Touch

Marcin Szwed, Knarik Bagdasarian,  
and Ehud Ahissar\*

Department of Neurobiology  
The Weizmann Institute  
Rehovot 76100  
Israel

## Summary

**Mammals acquire much of their sensory information by actively moving their sensory organs. Yet, the principles of encoding by active sensing are not known. Here we investigated the encoding principles of active touch by rat whiskers (vibrissae). We induced artificial whisking in anesthetized rats and recorded from first-order neurons in the trigeminal ganglion. During active touch, first-order trigeminal neurons presented a rich repertoire of responses, which could not be inferred from their responses to passive deflection stimuli. Individual neurons encoded four specific events: whisking, contact with object, pressure against object, and detachment from object. Whisking-responsive neurons fired at specific deflection angles, reporting the actual whiskers' position with high precision. Touch-responsive neurons encoded the horizontal coordinate of objects' position by spike timing. These findings suggest two specific encoding-decoding schemes for horizontal object position in the vibrissal system.**

## Introduction

Touch and vision are active processes (Ahissar and Arieli, 2001). Eyes, fingers, and whiskers move as they scan the external world and palpate objects. These movements of the sensory organs determine the nature of the sensory input. Yet, the principles underlying sensory encoding have not been characterized so far under active conditions.

The vibrissal system of the rat is a convenient model for studying active sensing (Brecht et al., 1997; Carvell and Simons, 1990; Fanselow and Nicolelis, 1999; Gao et al., 2001; Hattox et al., 2002; Kelly et al., 1999; Kleinfeld et al., 1999, 2002; Krupa et al., 2001; Nicolelis et al., 1995; O'Connor et al., 2002; Prigg et al., 2002). To detect, localize, and perceive objects, rats scan the environment with their whiskers at about five to ten sweeps ("whisks") per second (Carvell and Simons, 1990; Welker, 1964). The mechanical interactions between each moving whisker and the environment is sensed by thousands of mechanoreceptors situated around the follicle-sinus complex (FSC) (Ebara et al., 2002; Rice et al., 1986), which provide input to 150–400 neurons in the trigeminal ganglion (NV) (Lichtenstein et al., 1990; Pali et al., 2000; Tracey and Waite, 1995). These neurons constitute the input stage of the vibrissal system.

Classical studies on encoding by NV neurons were

conducted using moving stimuli applied to stationary, passive whiskers (Gibson and Welker, 1983; Lichtenstein et al., 1990; Shoykhet et al., 2000; Zucker and Welker, 1969). These studies demonstrated that NV neurons exhibit either rapidly (RA) or slowly (SA) adapting responses to sustained whisker deflections, respond differently to different directions of whisker movements, and have different velocity sensitivities. However, during active touch, as opposed to passive touch, the forces operating on the mechanoreceptors in the FSC are determined not only by the forces operating on the external shaft of the whisker but also by the forces exerted on the FSC by the intrinsic muscles. The effect of these latter forces on vibrissal encoding was not evaluated so far, as accurate stimulus control with behaving rats is extremely difficult.

Encoding of sensory events during active touch was previously investigated only once. In that pioneering study, Zucker and Welker introduced a method for investigating active sensing in anesthetized rats (Zucker and Welker, 1969). With this method, referred to here as "artificial whisking," muscle-driven whisking-like movements are induced by applying electrical stimulation to the facial motor nerve (Brown and Waite, 1974). Zucker and Welker observed that presenting an object in the whisking path increased the number of responsive neurons and that the temporal reliability of the generated spike patterns was high. However, they did not conduct quantitative measurements of responses to active touch and did not study the principles of active encoding.

Here we used the artificial whisking paradigm, with online spike sorting to eliminate stimulation artifacts and fast video recording to monitor whisker movement. We first examined what information is conveyed by first-order neurons during an active touch cycle. Then, we investigated how first-order neurons encode a specific external variable—the horizontal coordinate of an object's position.

## Results

We induced trains of artificial whisking at 5 and 8 Hz by stimulating the facial motor nerve and tracked movement trajectories with a fast digital video camera (1000 frames/s [fps]) (see Experimental Procedures). The amplitudes of whisking movements ranged from 11.5° to 49.1° (median = 22.3°). Within a whisking train, the shape and velocity of whisker movement was constant, with a slight increase (<10%) in both resting and protracted positions during the first three whisking cycles (Figure 1B). When an object was introduced in a whisker's path (Figure 1A), the whisker touched it, pressed, bent, and then when the electrical stimulation stopped, bent back and retracted (Figure 1C). Times and angles of whisker-object contact were measured from recorded video frames (see Experimental Procedures).

## Neuronal Responses in NV

We recorded extracellularly from 80 NV neurons in urethane-anesthetized rats (see Experimental Procedures).

\*Correspondence: ehud.ahissar@weizmann.ac.il

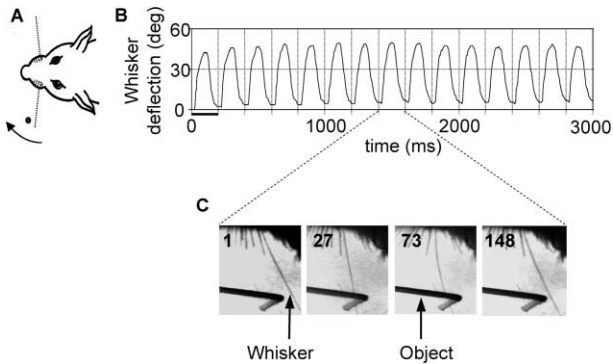


Figure 1. Artificial Whisking

(A) Experimental design. The rat whisks at an object (black dot). For clarity, only one whisker is shown on each side.

(B) Whisker trajectory of an entire 5 Hz artificial free-air whisking trial. Thick horizontal bar denotes one whisking cycle.

(C) Four video frames of a whisker resting, touching the object, bending, and retracting (from left to right). Numbers denote time elapsed from whisking onset. Images were stretched horizontally by 50% for clarity.

All units could be driven by manual stimulation of one of the large whiskers of the mystacial pad, and all had single whisker receptive fields. Of these 80 neurons, 61% displayed no spontaneous activity. The other 39% fired spontaneously at low rates ( $0.177 \pm 0.137$  spikes/s, mean  $\pm$  SD).

We classified these 80 neurons into four distinct categories, according to their responses to whisking in air and against an object (Table 1). “Touch cells” ( $n = 30$ ) responded only when the whisker touched the object. “Whisking cells” ( $n = 14$ ) responded only to whisking itself. “Whisking/Touch cells” ( $n = 15$ ) responded both when the whisker touched the object and to whisking itself. “High Threshold cells” ( $n = 21$ ) responded to passively applied rapid deflections (“passive stimulation”) but not to touch or whisking.

**Touch and Whisking Cells**

Touch cells did not respond to whisking in air and fired only upon contact with an object. They could be further divided into subpopulations that became active at different phases of the whisking cycle (Figures 2A and 2C). “Contact cells” ( $n = 8$ ) fired shortly after the whisker touched the object. “Pressure cells” ( $n = 11$ ) also started firing after contact but at longer delays and continued to fire as long as the whisker was pressing against the

object. “Detach cells” ( $n = 6$ ) fired only when the whisker started to retract and detach from the object. “Contact/ Detach cells” ( $n = 5$ ; shown in Figure 2 panels B and C only) exhibited two response components, one like that of Contact cells and one like that of Detach cells. Pressure cells differed from the remaining Touch cells both in response duration (Figure 2B) and response latency ( $p < 0.0001$ , Mann-Whitney test, see Table 1 for details).

Whisking cells responded only to whisking. These cells ( $n = 14$ ) fired the same way regardless of whether or not the whisker touched an object (Figure 3A). Five whisking cells exhibited short, phasic responses ( $< 20$  ms; inset of Figure 3A, orange) and nine exhibited long, tonic responses ( $> 80$  ms; magenta). Figure 3C depicts raster plots of three phasic and one tonic Whisking cells (from left to right), plotted against time.

Whisking/Touch cells ( $n = 15$ ) responded both to whisking and to touch (Figure 3B). When an object was present in the whisker’s path, these cells fired upon whisking onset and fired additional spikes upon touch (Figure 3B, red). During free-air whisking, three Whisking/ Touch cells exhibited long, tonic ( $> 80$  ms; inset of Figure 3B, magenta) responses, and 12 cells exhibited short, phasic ( $< 40$  ms; orange) responses. The majority (8 of 12) of these phasic cells fired long, tonic bursts upon touch (Figure 3B, red). The proportion of phasic/tonic

Table 1. Types of Trigeminal Ganglion Neuronal Responses

Active Response Type	n	Passive Response Type (%) <sup>a</sup>		Description of the Active Response Type	Duration (ms) <sup>b</sup>	Delay (ms) <sup>c</sup>
		SA	RA			
Touch	30	42%	58%	Neurons respond only to touch and fire:		
Contact	8	17%	83%	Briefly right after whisker touches the object	$16.4 \pm 8.8$	2–5 (2)
Pressure	11	100%	0%	Long trains as long as whisker presses at object	$118.2 \pm 17.4$	9–34 (15)
Detach	6	33%	67%	Briefly when the whisker detaches from object	$23.8 \pm 8.1$	14–2 (8)
Contact/Detach	5	0%	100%	Briefly both when whisker touches (+) and detaches (–) from object	$14.6 \pm 2.0$ (+) $15.5 \pm 8.2$ (–)	2–4 (2) (+) 27–6 (13) (–)
Whisking	14	50%	50%	Neurons respond only to whisking	$75.1 \pm 55.0$	3–140 (25)
Whisking/Touch	15	28%	72%	Neurons respond both to touch and whisking	$36.8 \pm 44.3$	2–102 (5)
High Threshold	21	40%	60%	Neurons unresponsive to artificial whisking: Respond only to strong mechanical stimulation		
Total	80	40%	60%			

<sup>a</sup>Passive response was tested for 62 of the 80 cells.

<sup>b</sup>Duration: Duration of the entire response (measured from the PSTH, as the period in which the response was larger than background activity), at 5 Hz whisking and protraction duration of 100 ms; mean  $\pm$  SD.

<sup>c</sup>Delay: For Pressure and Contact cells and for contact responses of Contact/Detach cells, delays were calculated from the time of whisker-object encounter until half peak of the rising edge of the PSTH. For Detach cells and detach responses of Contact/Detach cells, delays were calculated from the time of half peak of the rising edge of the PSTH to complete detachment of whisker from object. For Whisking cells, delays were calculated from whisking onset. Ranges and (medians) are depicted.

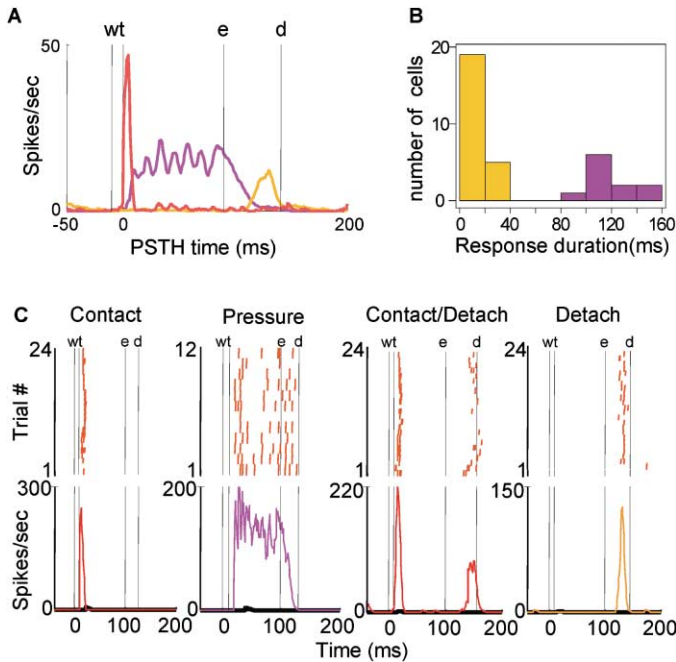


Figure 2. Touch Cells

(A) Average PSTHs of Contact (red,  $n = 8$ ), Pressure (magenta,  $n = 11$ ), and Detach (orange,  $n = 6$ ) cells, triggered on whisker-object contact. Vertical lines denote time of whisking onset (w), touching of object by the whisker (t), end of muscle contraction (e), and detachment of whisker from object (d). w, e, and d are population averages (touch occurred  $6.5 \pm 4.7$  ms after protraction onset, and detachment occurred  $43.1 \pm 3.3$  ms after end of muscle contraction). Modulation of Pressure cells' responses is a result of stimulus-locked modulation (see Results).

(B) Histogram of response durations of individual Touch cells (5 Hz whisking, 200 ms long cycle): Pressure cells, magenta; Contact, Detach, and Contact/Detach cells, orange. For Contact/Detach cells ( $n = 5$ ), the contact and detach responses were treated separately.

(C) Rasters (top panels) and PSTHs (bottom panels), triggered upon whisking onset, of (from left to right) a single Contact, Pressure, Contact/Detach, and Detach cell, with (PSTH, colored) and without (PSTH, black) an object present. PSTHs represent averages over four cycles in each trial.

cells and the response latencies differed for Whisking and Whisking/Touch cells ( $p = 0.04$  and  $= 0.01$ , respectively, Mann-Whitney, see Table 1 for details).

Two Whisking/Touch, two Whisking, three Pressure, one Contact, and one Contact/Detach cells were re-tested using the same protocol but with 8 Hz whisking (protraction duration changed from 100 to 62.5 ms). Response patterns and latencies of all cells remained unchanged. For Touch cells tested with an object present, spike counts per cycle decreased at 8 Hz by  $27\% \pm 20\%$ . For Whisking and Whisking/Touch cells tested during whisking in air, spike counts per cycle decreased at 8 Hz by  $28\% \pm 19\%$ .

#### Responses to Passive Deflection Stimulation

As a first step toward a comparison between passive and active sensing, we also recorded, for 62 of the 80 neurons, responses to passive computer-controlled for-

ward/backward deflections. We classified cells as slowly adapting (SA) and rapidly adapting (RA) (for details, see Experimental Procedures). Thirty seven (60%) cells were RA, and 25 (40%) were SA. Interestingly, the four types of cells: Touch, Whisking, Whisking/Touch, and High Threshold, contained similar proportions of RA and SA cells ( $p = 0.79$ , Kruskal-Wallis). Adaptivity could partially predict the active response subtype. Among Touch cells, Pressure cells were all SA, while Contact, Contact/Detach, and Detach cells were predominantly RA (13/16;  $p = 0.01$ , Kruskal-Wallis). Among Whisking and Whisking/Touch cells, tonic cells were more likely to be SA (5/8), while phasic cells were predominantly RA (8/9;  $p = 0.036$ , Mann-Whitney). Table 1 contains percentages of SA and RA cells in all cell types and subtypes.

We also examined whether a cell's response during active whisking can be predicted by its sensitivity to the direction of passive deflection. For example, it might

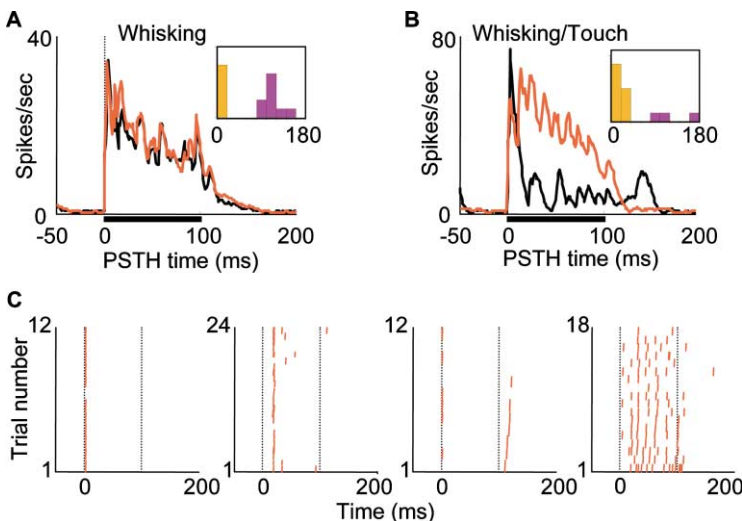


Figure 3. Whisking and Whisking/Touch Cells

Average responses of (A) Whisking cells ( $n = 14$ ) and (B) Whisking/Touch cells ( $n = 15$ ) to free-air whisking (black) and to whisking against an object (red). Insets show the distribution of response durations of these cells to free-air whisking. Black line on x axis shows duration of whisker protraction. (C) Three phasic and one tonic Whisking cell (from left to right)—raster plots during free-air whisking triggered upon whisking onset plotted against time. Dashed vertical lines denote protraction onset and offset time.

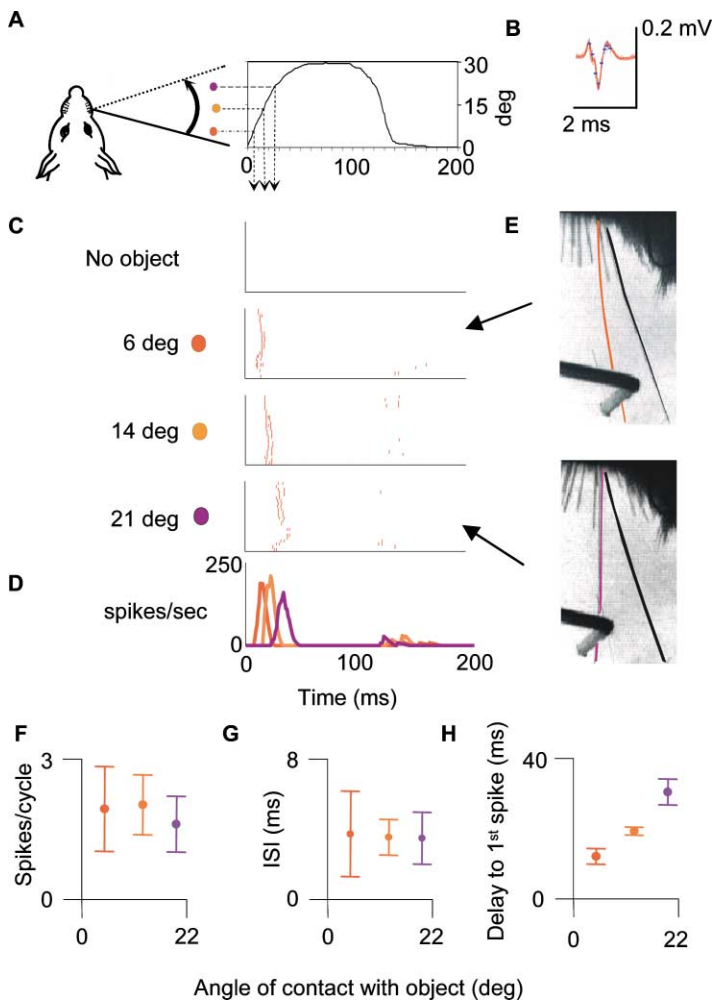


Figure 4. Encoding of Horizontal Object Position by a Contact/Detach Cell

(A) Trajectory of whisker movement determined from sequential video frames and angular object positions (circles of various colors) projected onto that trajectory. Contact times are indicated by dashed lines. (B) Superimposed samples of the cell's spike (red,  $n = 16$ ). Blue marks indicate the sorting template. (C) Raster plots of single spikes during 24 trials in which the object (vertical pole) was absent ("No object") or positioned at various angles in the whisking field. (D) PSTHs of the responses in (C). (E) Superimposed video images of the whisker in the resting position (black) and while touching the object (red, magenta). (F–H) Spike count per cycle (F), interspike intervals (G), and delays from protraction onset to first spike (H), for the various angles of whisker-object contact (mean  $\pm$  SD).

seem logical that Contact cells should be more sensitive to backward deflections (i.e., passive deflection offset) and Detach cells to forward deflections (i.e., passive deflection onset). To answer this question, we calculated DirIndex (spikes during forward deflection/spikes during backward deflection) for the 62 neurons tested quantitatively with passive deflections. Twenty cells (32%) responded only to protraction (DirIndex = 0). The ratios of forward/backward responses for the remaining 42 cells (68%) ranged from 0.08 to 2.51. We found no significant difference in directionality between the four main cell types (Touch, Whisking, Whisking/Touch, and High Threshold;  $p = 0.48$ , Kruskal-Wallis) and Touch cell subtypes (Contact, Pressure, Detach, and Contact/Detach;  $p = 0.22$ ).

For 70 of 80 cells recorded, we also assessed how selectively they responded to passive, manual deflections of the whisker in four directions (up, down, forward, and backward). We found no significant difference in direction sensitivity between any of the four main cell types nor between different Touch cell subtypes ( $0.18 < p < 0.98$ , Kruskal-Wallis tests).

#### Encoding of Horizontal Object Position

During tactile discrimination behavior, rats appear to utilize information available in one or a few whisking

cycles (Carvell and Simons, 1990, 1995). Thus, we examined encoding by neuronal variables that are well defined within a single whisking cycle: delay from protraction onset to the first spike, spike count per cycle, and instantaneous firing rate (assessed by the average interspike interval in a cycle).

Each Touch and Whisking/Touch neuron was recorded while an object was introduced at three different horizontal positions. Figure 4 depicts the paradigm (panel A), spike shape (panel B), and encoding scheme (panels C–H) of one Contact/Detach neuron. This neuron did not respond during free-air whisking (Figure 4C, No object) but did respond with a short burst upon contact with the object (Figures 4C and 4D). It encoded horizontal object position by time: the cell's firing times, relative to whisking onset, were reliable indicators of horizontal object position ( $R^2 = 0.85$ , Figure 4H). In contrast, the spike counts and instantaneous firing rate of this cell did not provide any information about object position ( $R^2 = 0.06$  and  $R^2 = 0.01$ , Figures 4F and 4G, respectively).

We compared the amount of information conveyed by temporal and rate coding by computing coefficients of determination ( $R^2$ ) between horizontal contact angles and the (1) delay to the first spike, (2) spike count per cycle, and (3) average interspike interval per cycle. Fig-

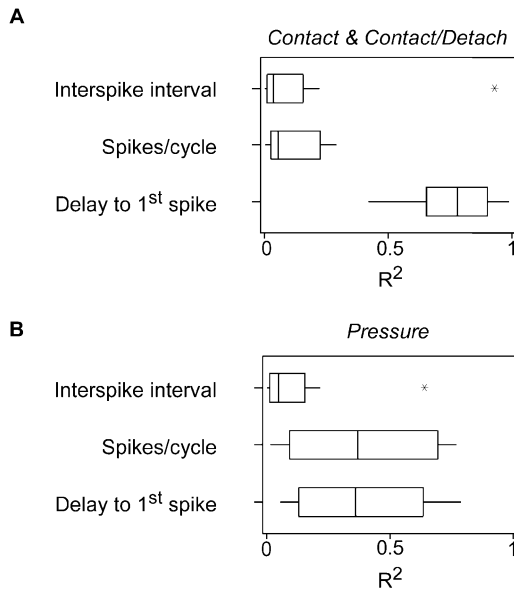


Figure 5. Encoding of Horizontal Object Position by Touch Cells  
Coefficients of determination ( $R^2$ ) for individual Touch neurons' linear regressions of three neuronal variables against three angles of whisker-object contact. Box plots show  $R^2$  distributions for 11 Contact and Contact/Detach neurons (A), and nine Pressure neurons (B). Boxes represent the first (25%) to third (75%) quartile values, line inside box indicates median, horizontal lines indicate range. Outliers ( $>3$  interquartile values from median) are indicated by stars. Regressions were not computed for four neurons for which the range of horizontal object angles was very small ( $<5^\circ$ ).

Figure 5 shows the median and range of  $R^2$ , for each of these variables, for the Contact, Contact/Detach, and Pressure cells of our sample. For Contact and Contact/Detach cells, the temporal variable contained significantly more information than the two rate variables ( $p < 0.001$ , Kruskal-Wallis; Figure 5A). For Pressure cells, delay to first spike and spike count conveyed a similar amount of information, and both these codes conveyed more information than interspike interval ( $p = 0.024$ , Kruskal-Wallis; Figure 5B).

### Encoding of Whisker Position

We asked how much information about whisker position is conveyed by Whisking and Whisking/Touch cells. Do they report only the onset and duration of movement? Or perhaps, as previously suggested (Fee et al., 1997), they provide specific phase information that allows reconstruction of the whisker's trajectory? To answer this question, we computed the temporal phase fields of Whisking and Whisking/Touch cells ( $n = 27$ ), i.e., the range of temporal phases along the whisking cycle in which they emitted spikes (see Experimental Procedures). While about half of the cells began firing in the first 1/9 of the protraction cycle, firing times of the entire population covered the entire protraction period (0–100 ms), with six cells firing also during the retraction period (Figure 6A). This phase encoding was reliable across trials (the SD of onset latencies across all trials of an individual cell was  $2.02 \pm 2.9$  ms, Figure 6B; see also Figure 3C).

In active sensing, the temporal phase of sensor movement is directly related to its spatial position. To quantify the encoding of spatial angles by Whisking and Whisking/Touch cells, we computed angle fields, i.e., the ranges of whisker angles for which they emitted spikes (Figure 6C), and spatial phases, i.e., the fractions of whisking amplitude signaled by these spikes (Figure 6E). As expected from the distribution of temporal phase fields (Figure 6A), angle fields of our sample were distributed across the entire range of whisking angles tested with these neurons ( $0^\circ$ – $30^\circ$ ) and covered the entire range of spatial phases (0–1). Their onset position was highly reliable across trials (SD of onset angle and phase across all trials of an individual cell was  $0.58^\circ \pm 0.91^\circ$  and  $0.018 \pm 0.003$ , Figures 6D and 6F, respectively). Whether these cells primarily encode temporal phase of whisker movement, absolute whisker angle, or spatial phase of whisker movement should be resolved in experiments in which whisking timing, amplitude, and trajectory are independently manipulated.

### Stimulus-Locked Modulations

In 21 out of 39 cases, detailed analysis of whisking trajectories revealed whisker micromovements of  $0.3^\circ$  to  $2.6^\circ$  (median =  $0.9^\circ$ ) superimposed on the main movement pattern. These movement modulations had the same frequency (83 Hz) as that of the electrical current pulses used to drive whisking (see Experimental Procedures) and were visible from the moment the whisker approached maximum deflection until the end of the electrically driven whisker protraction. Pressure, tonic Whisking, and tonic Whisking/Touch cells exhibited 83 Hz modulations in their responses (Figures 2 and 3), which were phase locked to the whisker micromovements. The modulation depth  $[(\max - \min)/(\max + \min)]$  of the response was  $0.47 \pm 0.29$  for the Pressure cells ( $n = 11$ ) and  $0.63 \pm 0.32$  for the tonic Whisking and Whisking/Touch cells ( $n = 9$ ) examined. This modulated component of the response was not due to artifactual "spikes" spilling into the single-unit window of the spike sorter, but a sensory response to the whisker micromovements (see Experimental Procedures).

### Discussion

We found that during active touch in anesthetized rats, individual NV neurons encoded four specific events: whisking, contact with object, pressure against object, and detachment from object. Whisking neurons encoded whiskers' position with high precision by firing at specific deflection angles. Touch neurons encoded the horizontal object position by spike timing relative to whisking onset.

These results are consistent with those of Zucker and Welker, who observed a segregation between neurons responding to whisking and neurons responding to touch in NV (Zucker and Welker, 1969), and with those of Brown and Waite, who observed that such a segregation is still evident in the ventrobasal thalamus (Brown and Waite, 1974). The repertoire of responses revealed by our experiments can probably be accounted for by the rich repertoire of mechanoreceptors in the whisker follicle, their type, location along the follicle, and the

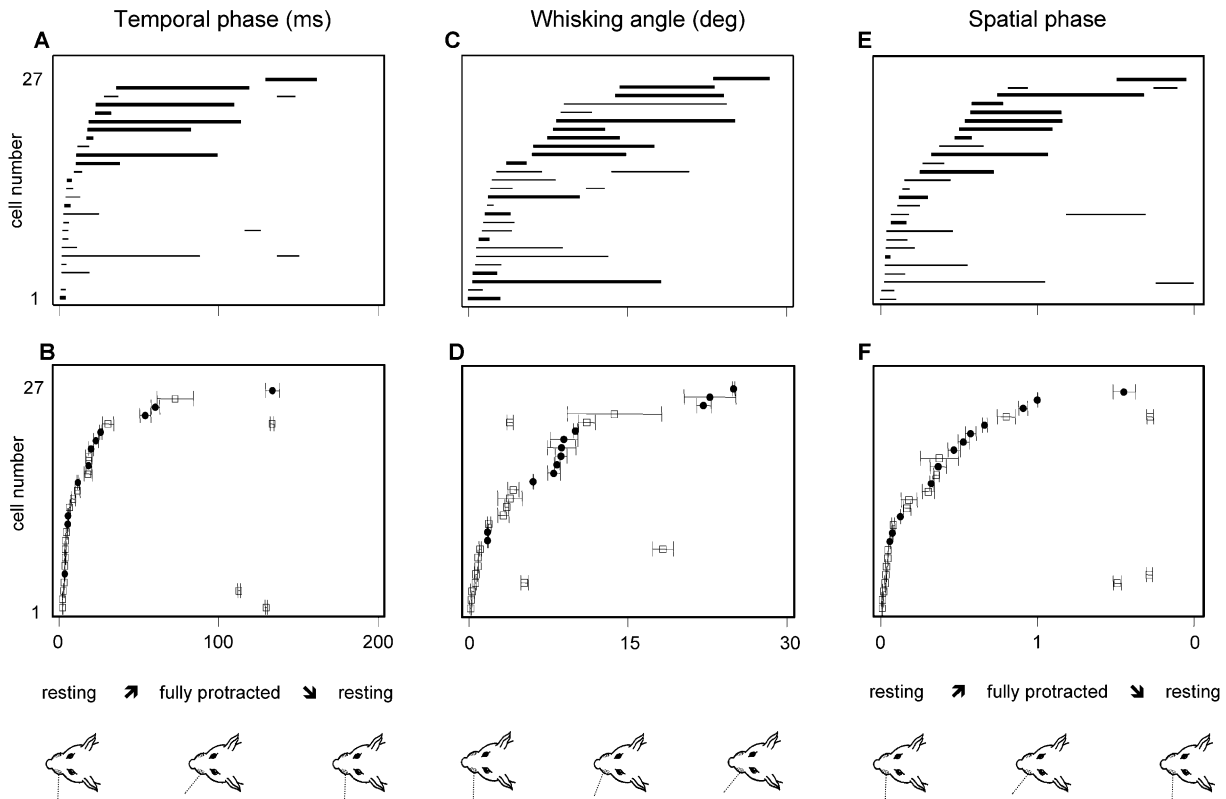


Figure 6. Encoding of Whisker Position by Whisking and Whisking/Touch Cells During Free-Air Whisking

(A, C, and E) Firing fields. Each horizontal line represents temporal phases (A), angles (C), and spatial phases (E) along the whisking cycle in which a Whisking (thick line) or Whisking/Touch (thin line) cell was active (see Experimental Procedures). Temporal phase is the delay from protraction onset, angle is measured from resting position, and spatial phase is the angle divided by protraction amplitude. (B, D, and F) Firing onsets. Each plot depicts temporal phases (B), angles (D), and spatial phases (F) at which Whisking (filled circles) or Whisking/Touch (outlined squares) fired their first spike. Error bars represent standard deviation. Note that with low firing rates the average delay of the first spike can be significantly larger than the delay at which the PSTH reaches its half-height (see Discussion in Sosnik et al., 2001). The rows in which two lines (A, C, and E) or symbols (B, D, and F) are present represent cells that fired both during protraction and retraction. Cells are ordered by onset phase (A, B, E, and F) or angle (C and D), independently for each panel.

configuration of their surrounding tissue (Ebara et al., 2002; Rice et al., 1986). In fact, this anatomical repertoire appears to allow even richer functional repertoire, which could most likely be exposed with different sensory tasks. For example, it is likely that Pressure cells, which have long, tonic responses and that can phase lock to very small changes in stimulus intensity (Figure 2, see also Gottschaldt and Vahle-Hinz, 1981), will exhibit a richer repertoire of response while scanning various textures. Also other cell types, including our “High Threshold” neurons, might exhibit additional response patterns depending on texture parameters, scanning velocity, and the radial distance of contact. Thus, a type attributed to an NV cell in this study does not represent the sole function of the cell. Rather, it describes a particular type of information conveyed by this cell in a given context (object location in this case). In general, we do not think that neurons can be classified according to rigid invariant types. We believe that a neuron’s response always depends on the context; in the case of NV neurons, the major contextual factors appear to be the movement profile of the whisker and the nature of the environment.

#### Artificial versus Natural Whisking

The responses of NV neurons are unlikely to be affected by the state of anesthesia (Maggi and Meli, 1986). There are, however, other differences between our experimental conditions and natural ones, which probably affect the exact mechanics of whisker movement and its interactions with the environment. In awake whisking animals, sympathetic and parasympathetic activation monitor blood supply to the follicle (Fundin et al., 1997), which might affect not only its geometrical movement parameters but also the sensitivity of mechanoreceptors (Gottschaldt et al., 1973); whether similar effects occur during electrical stimulation of the facial nerve is not yet known. In awake animals, whisker retraction probably involves activation of extrinsic facial muscles (Berg and Kleinfeld, 2003), while in our artificial paradigm retraction is passive. With artificial whisking, a small stimulus-locked component (83 Hz in our case) is superimposed on the main protraction trajectory. Finally, in awake animals, whisking patterns are not constant—they vary across cycles (Carvell and Simons, 1990; Gao et al., 2001) and between whisking bouts (O’Connor et al., 2002). Thus, although the principle of muscle-driven whisker

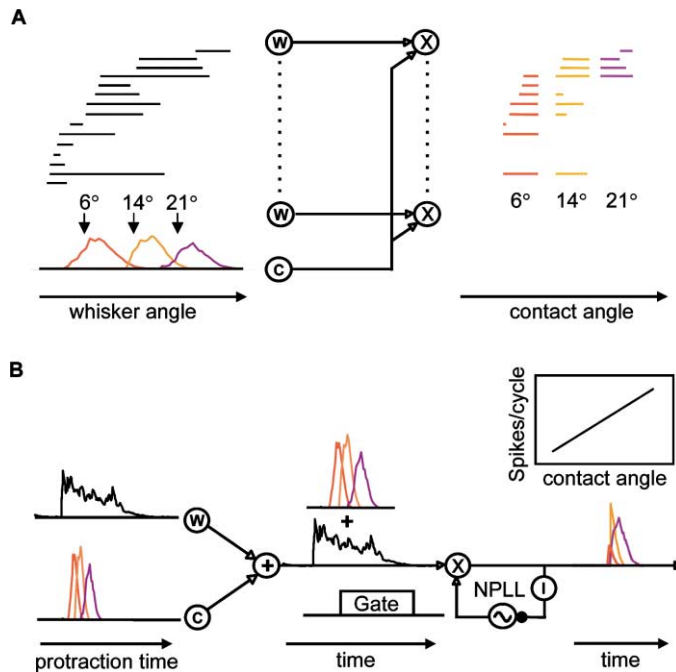


Figure 7. Possible Encoding-Decoding Schemes for Horizontal Object Position

(A) Spatiotemporal scheme. Outputs of Whisking cells (W, from Figure 6C) and a Contact cell (C, from Figure 4D) are fed separately into an array of cells that function as coincidence or phase detectors (X). Horizontal object positions are coded, from posterior to anterior, by red, orange, and magenta (as in Figure 4). The output of the detectors' array provides a spatial code of horizontal object position (colored firing profiles).

(B) Temporal scheme. Outputs of a population of Whisking cells (W, from Figure 4A) and a Contact cell (C, from Figure 4D) are summed and then fed into a thalamocortical NPLL circuit of the paralemniscal pathway. Temporal dispersion along this pathway broadens the responses. The NPLL is composed of a thalamic phase detector (X; implemented by a set of "relay" cells), cortical inhibitory neurons (I), and cortical oscillators (~). The thalamic neurons transfer only those input spikes that coincide with the cortical gating feedback (black pulse). Thus, responses to more posterior locations, which decay earlier than those to more anterior positions, will yield less spikes. As a result, horizontal object position is encoded by the spike count of the thalamic neurons (Ahissar and Arieli, 2001; Ahissar et al., 2000; Ahissar and Zacksenhouse, 2001).

movement and the basic pattern of movement trajectory are preserved in our experiments (compare, for example, Figure 1A with Figure 2 in Gao et al., 2001), the details of movements and mechanical interactions probably differ. However, while whisking movements during artificial and natural conditions may differ in detail, the principles by which movement properties are encoded in neuronal responses should be similar.

#### Possible Encoding-Decoding Schemes

According to our results, horizontal object position (in whisker-related coordinates) is encoded by (1) coincident firing of individual Whisking and Contact cells, and (2) the temporal interval between onset firing of Whisking cells and firing of Contact cells.

An efficient way to understand these encoding schemes would be to ask: how could the encoded information be extracted, or read out, by downstream neuronal circuits? Temporal coincidences between Whisking and Contact cells could be read out by an array of coincidence (Jeffress, 1948) or phase (Ahissar, 1998) detectors, i.e., cells whose outputs depend sharply or gradually, respectively, on the temporal phase difference between their inputs (Figure 7A). When fed by an array of Whisking cells whose phase fields span the protraction period (Figure 7A, left) and by a unified signal of Contact cells, this array of detector cells should generate an output whose spatial firing profile would be specific for every contact angle (Figure 7A, right). Decoding accuracy in this spatiotemporal scheme would be impaired by any addition of temporal dispersion, which suggests that such a decoding should be performed by the lemniscal pathway of the vibrissal system, whose neuronal responses are tightly locked to stimulus timing (Ahissar et al., 2000; Diamond et al., 1992).

The alternate encoding scheme, which is based on interval coding, could be decoded by neuronal phase-locked loops (NPLLs; Ahissar, 1998) of the paralemniscal system (Ahissar and Arieli, 2001; Ahissar and Zacksenhouse, 2001; Kleinfeld et al., 1999) (Figure 7B). NPLLs would receive the summed activity of Whisking and Contact neurons, detect the temporal interval between them, and translate it to a spike-count code. This temporal-to-rate transformation mechanism is described in detail elsewhere (Ahissar, 1998). Briefly, the cortical oscillators lock to the firing of Whisking cells with a certain phase lag. A gating signal sent from the cortex to thalamic neurons ("gate") would select the later period of NV firing. The more anterior positions, whose contact signals appear in a later period of protraction, would thus produce higher spike counts (Ahissar, 1998; Ahissar and Zacksenhouse, 2001) (see output of NPLL in Figure 7B). In this temporal scheme, the decoding process is facilitated by the inherent temporal dispersion of the paralemniscal system, which broadens the input signals and, thus, increases sensitivity to phase differences (Ahissar and Arieli, 2001; Ahissar and Kleinfeld, 2003; Ahissar et al., 2000, 2001; Ahissar and Zacksenhouse, 2001; Sosnik et al., 2001).

Decoding of horizontal object position would probably benefit from a combination of these two schemes, which seem to provide complementary sets of working ranges and resolutions. Cooperation between these two mechanisms might even be required to allow the reading of the decoded spatial code of the spatiotemporal scheme—since the spatial code is valid only during the protraction periods of single whisking cycles, it must be read by a mechanism that can phase lock to the whisking cycle. Such cooperation might explain why cortical cells exhibit phase coding during whisking in free air (Fee et al.,

1997), while output cells of the spatiotemporal scheme are expected to remain silent if no contact occurs (Figure 7A). Phase coding during whisking in free air is indeed expected in the cortex when assuming an integration of temporal and spatiotemporal schemes (Ahissar and Kleinfeld, 2003).

### Which Receptors Provide the Whisking and Touch Inputs?

There are at least six types of mechanoreceptors in the whisker FSC. These receptors are distributed across all levels of the FSC starting from the epidermal rete ridge collar (RRC), through the outer and inner conical body (OCB and ICB), the ringwulst (Rw), the ring sinus (RS) to the cavernous sinus (CS) (Ebara et al., 2002; Rice et al., 1986, 1993). The types of events to which a particular receptor is sensitive should be determined by the type of the receptor and its location in the FSC. Our results indicate that the receptive event space of an individual NV cell is restricted and well defined, which is not surprising, since each ganglion cell receives input from only one precisely localized receptor type (Ebara et al., 2002).

Why do not all of the mechanoreceptors in the FSC respond to free-air whisking? We speculate that the type of a receptor's response depends primarily on its location in relation to the blood sinuses (RS and CS; see Figure 1 in Ebara et al., 2002). Receptors that are situated between the blood sinuses and the whisker shaft should be much less affected by free-air whisking, when there should be almost no tension between the blood sinuses and the whisker shaft. These receptors, however, would be activated by touch; when the whisker touches an object during movement, it presses against the blood sinuses opposite to the direction of the force applied by the intrinsic muscles. In contrast, receptors located in the RRC, OCB, and ICB should be sensitive to whisking in free air. They are not protected by blood sinuses and therefore should respond to the tension that develops between the moving follicle and the surrounding tissue. Consistent with this hypothesis is the finding that the RRC Merkel receptors and the ICB lanceolate receptors are the only receptors distributed preferentially along the planes parallel to the direction of whisker movement (Ebara et al., 2002); the latter are present only in whisking species (Mosconi et al., 1993; Ebara et al., 2002). Which of these receptors are sensitive to whisking only and which to whisking and touch probably depends on additional factors, such as their anatomical type and orientation. Since the upper sections of the follicle (the RRC, OCB, and ICB) are innervated by the superficial vibrissal nerve while the lower sections, i.e., the RS and CS, by the deep vibrissal nerve (Rice et al., 1986; Waite and Jacquin, 1992), it might be that the Whisking responses are conveyed mostly by the superficial nerve while Touch responses are conveyed by the deep nerve.

The extent to which the blood sinuses isolate the receptors must depend on the parameters of movement—the isolation is expected to decrease with increased accelerations. Furthermore, when the whisker shaft is used as a lever to move the follicle against static muscles, as in passive deflections, the rules for receptor activation should be different. These two factors might

explain why cells that were not activated by whisking were activated by passive deflection stimuli, as these stimuli are of high acceleration (Sosnik et al., 2001) and act directly on the whisker's shaft, thus bypassing the isolation provided by the blood sinuses.

### Difference between Passive and Active Responses

In classical studies, NV neurons have usually been classified according to their responses to sustained passive deflections (Lichtenstein et al., 1990; Shoykhet et al., 2000; Zucker and Welker, 1969). As a first step toward understanding the relation between active and passive responses, we applied passive deflection stimuli that would yield whisker movements similar to active movements, i.e., forward-backward deflections of amplitude roughly similar to the artificial whisking amplitude (see Experimental Procedures). We found out that responses of a given NV cell to these stimuli provide only limited information about its responses in the active mode. For example, knowing that a cell is RA allows one to predict that its active response will most likely be phasic but not whether it reports whisking or touch in the active mode.

Possibly, an exhaustive set of passive deflection tests might provide more information about active encoding by first-order neurons. For example, phase encoding by Whisking cells might be related to their velocity sensitivities (Gibson and Welker, 1983; Shoykhet et al., 2000), and the switch from phasic to tonic firing of Whisking/Touch cells might be related to both their velocity and directional sensitivities (see Figure 1 in Lichtenstein et al., 1990). It should be emphasized, however, that the conditions during active protraction, when the FSC is actively pulled by intrinsic muscles, cannot be reproduced by passive deflection stimuli that act only on the external shaft of the whisker. Thus, it is most likely that at least some response patterns can be observed only in the active mode.

Understanding of sensory computation depends crucially on knowing the input signals. This study demonstrates the necessity of examining vibrissal input signals in the active mode. It remains to be discovered whether a similar necessity holds for other sensory modalities, such as manual touch or vision.

### Experimental Procedures

#### Animal Preparations and Electrophysiology

Experiments were performed on 21 male Albino Wistar rats weighing 200–300 g. Animal maintenance, manipulations, and surgeries were conducted in accordance with NIH standards. Surgical procedures were performed under general anesthesia with intraperitoneal injection of urethane (1.5 g/kg). Supplemental doses of anesthesia (10%) were administered when required. Atropine methyl nitrate (0.3 mg/kg, i.m.) was administered to prevent respiratory complication. Anesthetized animals were secured in a stereotaxic device (SR-6; Narishige; Japan). Body temperature was maintained at 37°C. An opening was made in the skull overlying the left trigeminal ganglion, and tungsten microelectrodes (0.5–1 M $\Omega$ , Alpha Omega Engineering, Israel) were lowered according to known stereotaxic coordinates of NV (Shoykhet et al., 2000) until units drivable by whisker stimulations were encountered. Standard methods for single-unit recordings were used (Sosnik et al., 2001). Single-units were sorted by spike templates. We considered units as single only if they had homogeneous spike shapes that did not overlap with other units or noise and if they exhibited refractory periods of >1 ms in their autocorrelation

histograms. Artifacts produced by electrical stimulation were isolated by the online spike sorter (MSD-3.21; Alpha-Omega Engineering) and removed from unit recordings.

#### Artificial Whisking

We induced artificial whisking by stimulating the buccal motor branch of the facial nerve (Semba and Egger, 1986). The nerve was cut, its distal end mounted on bipolar silver electrodes, and was kept moist by brief washes with warm saline between periods of stimulation. We applied bipolar rectangle electrical pulses (0.5–4.0 V, 83 Hz, 40  $\mu$ s duration; parameters adapted from Brown and Waite, 1974) through an isolated pulse stimulator (2 x ISO-Flex; A.M.P.I. Israel). All stimulation parameters except the voltage were identical in all recordings. The stimulation voltage was adjusted (within the range of 0.5–4 V) at the beginning of each recording session to the minimal value that reliably generated the maximal possible movement amplitude. Artificial whisking was composed of active protraction and passive retraction; components of active retraction, such as those recently observed (Berg and Kleinfeld, 2003), were not induced.

The electrical stimulation often induced whisker micromovements superimposed on the main movement pattern. Tonic neurons also exhibited 83 Hz modulations in their responses, which were phase locked to the whisker micromovements (see Results). This modulated component of the response was not due to artifactual “spikes” spilling into the single-unit window of the spike sorter because (1) artifactual “spikes” were isolated by a dedicated template, (2) spike isolations were monitored online and examined offline (no artifactual “spikes” were observed in single-unit windows), and (3) spikes of individual cells did not occur at the moment of nerve stimulation but rather with a constant delay that matched the sensory delay of the main response. In two experiments, we varied the motor nerve stimulation frequency in the 50–100 Hz range; the micromovement frequency tracked the stimulation frequency of the nerve, and the modulations of the neuronal response remained locked to modulations of whisker movement.

#### Histology

In four pilot experiments, at the end of the recording session, electrolytic lesions were induced by passing currents (10  $\mu$ A, 2 x 2 s, unipolar) through the tips of the recording electrodes in order to verify the location of the electrode tip in the ganglion. The brains were then cut and stained for cytochrome oxidase (Haidarliu and Ahissar, 1997). Lesions located in the ganglion could be clearly seen. In subsequent experiments, histological procedures were not conducted, since the anatomic location of the ganglion and the highly typical responses of the primary afferent cells precluded another source of recordings (Shoykhet et al., 2000; Zucker and Welker, 1969).

#### Experimental Paradigms

We induced 5 Hz (and in some cases also 8 Hz), 50% duty cycle (i.e., muscle-contraction period/cycle duration) trains of artificial whisking followed by intertrain intervals of 2 s in blocks of 12 to 24 trains (trials). We recorded whisker movements at 1000 frames/s with a fast digital video camera (MotionScope PCI 1000; Redlake; San Diego, CA). Video recordings were synchronized with neurophysiological data with 1 ms accuracy. Blocks of free-air artificial whisking were interleaved with blocks of artificial whisking against an object and blocks of mechanical (passive) stimulations. For the first 16 experiments (47/80 assessed neurons), trains lasted 3 s, and for blocks of artificial whisking against an object, a vertical pin-shaped object (Figures 1A and 1C) was introduced into the whisking field after five cycles of free-air whisking and retracted after five additional cycles. In the subsequent seven experiments (33/80 assessed neurons), trains lasted 2 s, and in object blocks, the object was positioned before train onset. For all experiments, the distance of the object from the skin was 80%–90% of whiskers' length.

For mechanical (passive) stimulation, a mechanical stimulator was attached to the whisker 4 mm from the skin and forward/backward pulses (1 Hz, amplitude = 0.9 mm, rise/fall time = 5 ms, duty cycle = 50%, effective deflection angle = 13°) were applied (Haidarliu et al., 1999; Sosnik et al., 2001). We also determined qualitatively the

directionality of the response by pushing the whisker up, down, forward, and backward with a hand-held probe and listening to the audio feedback of the isolated unit.

#### Analysis of Neuronal Data

Trajectories of whisker movements were analyzed offline, with custom-written MATLAB applications. Statistical analysis was done with MINITAB (Minitab Inc), except for regressions, which were computed with MATLAB. For non-normally distributed data ( $p < 0.05$ ; Anderson-Darling), nonparametric tests were used to compare samples. All error bars indicate standard deviation. Raster plots and PSTHs (1 ms bins, smoothed by convolution with a triangle of area 1 and a base of  $\pm 10$  ms) were computed and examined for all trains of each cell. For quantitative analyses, four consecutive cycles were analyzed for each cell: cycles seven through ten of the 3 s trains and cycles four through seven of the 2 s trains. Average response latencies were computed from PSTHs as the delay from external events to 1/2 peak response. We analyzed neuronal encoding by computing delay to first spike, spike count per cycle, and average interspike interval, for each whisking cycle, as well as their means and SDs across trials (Sosnik et al., 2001). Delay to first spike and latency to 1/2 peak behaved similarly for Touch, Whisking/Touch, and Whisking neurons (paired t test,  $p = 0.95, 0.68, \text{ and } 0.54$ , respectively). The width of angle and phase fields of Whisking neurons were estimated from the PSTHs as the range of angles or phases for which the cell's response was higher than half of its maximal response.

To classify the cells' passive response type, we calculated Adaptation Index (AdIndex) = sustained response/onset response, where sustained and onset responses were the spike counts between 100–400 ms and 0–20 ms, respectively, from stimulus onset (background spikes were not subtracted). We classified cells with AdIndex = 0 as RA and those with AdIndex > 0 as SA. This classification is biased toward SA: a single spike fired in the 100–400 ms period was enough to classify a cell as SA.

#### Acknowledgments

We thank Amos Arieli, Shabtai Barash, Dori Derdikman, Per Knutsen, Ilan Lampl, Frank Rice, Daniel Simons, Jimmy Stehberg, and Phil Zeigler for helpful comments; Silvina Freund for graphic design; Naama Rubin for programming; Barbara Schick for editing; and Sebastian Haidarliu for assisting us with histology. This work was supported by research grants from the Irving B. Harris Foundation, Nella and Leon Benozzi Center for Neurosciences, the Israel Science Foundation grant #377/02-1, and the MINERVA Foundation, Germany. E.A. holds the Helen and Sanford Diller Family Professorial Chair of Neurobiology.

Received: May 29, 2003

Revised: August 18, 2003

Accepted: October 3, 2003

Published: October 29, 2003

#### References

- Ahissar, E. (1998). Temporal-code to rate-code conversion by neuronal phase-locked loops. *Neural Comput.* 10, 597–650.
- Ahissar, E., and Arieli, A. (2001). Figuring space by time. *Neuron* 32, 185–201.
- Ahissar, E., and Kleinfeld, D. (2003). Closed-loop neuronal computations: Focus on vibrissa somatosensation in rat. *Cereb. Cortex* 13, 53–62.
- Ahissar, E., and Zacksenhouse, M. (2001). Temporal and spatial coding in the rat vibrissal system. *Prog. Brain Res.* 130, 75–88.
- Ahissar, E., Sosnik, R., and Haidarliu, S. (2000). Transformation from temporal to rate coding in a somatosensory thalamocortical pathway. *Nature* 406, 302–306.
- Ahissar, E., Sosnik, R., Bagdasarian, K., and Haidarliu, S. (2001). Temporal frequency of whisker movement. II. Laminar organization of cortical representations. *J. Neurophysiol.* 86, 354–367.
- Berg, R.W., and Kleinfeld, D. (2003). Rhythmic whisking by rat: re-

- traction as well as protraction of the vibrissae is under active muscular control. *J. Neurophysiol.* 89, 104–117.
- Brecht, M., Preilowski, B., and Merzenich, M.M. (1997). Functional architecture of the mystacial vibrissae. *Behav. Brain Res.* 84, 81–97.
- Brown, A.W., and Waite, P.M. (1974). Responses in the rat thalamus to whisker movements produced by motor nerve stimulation. *J. Physiol.* 238, 387–401.
- Carvell, G.E., and Simons, D.J. (1990). Biometric analyses of vibrissal tactile discrimination in the rat. *J. Neurosci.* 10, 2638–2648.
- Carvell, G.E., and Simons, D.J. (1995). Task- and subject-related differences in sensorimotor behavior during active touch. *Somatosens. Mot. Res.* 12, 1–9.
- Diamond, M.E., Armstrong-James, M., Budway, M.J., and Ebner, F.F. (1992). Somatic sensory responses in the rostral sector of the posterior group (POm) and in the ventral posterior medial nucleus (VPM) of the rat thalamus: dependence on the barrel field cortex. *J. Comp. Neurol.* 319, 66–84.
- Ebara, S., Kumamoto, K., Matsuura, T., Mazurkiewicz, J.E., and Rice, F.L. (2002). Similarities and differences in the innervation of mystacial vibrissal follicle-sinus complexes in the rat and cat: a confocal microscopic study. *J. Comp. Neurol.* 449, 103–119.
- Fanselow, E.E., and Nicolelis, M.A.L. (1999). Behavioral modulation of tactile responses in the rat somatosensory system. *J. Neurosci.* 19, 7603–7616.
- Fee, M.S., Mitra, P.P., and Kleinfeld, D. (1997). Central versus peripheral determinants of patterned spike activity in rat vibrissa cortex during whisking. *J. Neurophysiol.* 78, 1144–1149.
- Fundin, B.T., Pfaller, K., and Rice, F.L. (1997). Different distributions of the sensory and autonomic innervation among the microvasculature of the rat mystacial pad. *J. Comp. Neurol.* 389, 545–568.
- Gao, P., Bermejo, R., and Zeigler, H.P. (2001). Whisker deafferentation and rodent whisking patterns: behavioral evidence for a central pattern generator. *J. Neurosci.* 21, 5374–5380.
- Gibson, J.M., and Welker, W.I. (1983). Quantitative studies of stimulus coding in first-order vibrissa afferents of rats. 1. Receptive field properties and threshold distributions. *Somatosens. Res.* 1, 51–67.
- Gottschaldt, K.M., and Vahle-Hinz, C. (1981). Merkel cell receptors: structure and transducer function. *Science* 214, 183–186.
- Gottschaldt, K.M., Iggo, A., and Young, D.W. (1973). Functional characteristics of mechanoreceptors in sinus hair follicles of the cat. *J. Physiol.* 235, 287–315.
- Haidarliu, S., and Ahissar, E. (1997). Spatial organization of facial vibrissae and cortical barrels in the guinea pig and golden hamster. *J. Comp. Neurol.* 385, 515–527.
- Haidarliu, S., Sosnik, R., and Ahissar, E. (1999). Simultaneous multi-site recordings and iontophoretic drug and dye applications along the trigeminal system of anesthetized rats. *J. Neurosci. Methods* 94, 27–40.
- Hattox, A.M., Priest, C.A., and Keller, A. (2002). Functional circuitry involved in the regulation of whisker movements. *J. Comp. Neurol.* 442, 266–276.
- Jeffress, L.A. (1948). A place theory of sound localization. *J. Comp. Physiol. Psychol.* 41, 35–39.
- Kelly, M.K., Carvell, G.E., Kodger, J.M., and Simons, D.J. (1999). Sensory loss by selected whisker removal produces immediate disinhibition in the somatosensory cortex of behaving rats. *J. Neurosci.* 19, 9117–9125.
- Kleinfeld, D., Berg, R.W., and O'Connor, S.M. (1999). Anatomical loops and their electrical dynamics in relation to whisking by rat. *Somatosens. Mot. Res.* 16, 69–88.
- Kleinfeld, D., Sachdev, R.N., Merchant, L.M., Jarvis, M.R., and Ebner, F.F. (2002). Adaptive filtering of vibrissa input in motor cortex of rat. *Neuron* 34, 1021–1034.
- Krupa, D.J., Matell, M.S., Brisben, A.J., Oliveira, L.M., and Nicolelis, M.A. (2001). Behavioral properties of the trigeminal somatosensory system in rats performing whisker-dependent tactile discriminations. *J. Neurosci.* 21, 5752–5763.
- Lichtenstein, S.H., Carvell, G.E., and Simons, D.J. (1990). Responses of rat trigeminal ganglion neurons to movements of vibrissae in different directions. *Somatosens. Mot. Res.* 7, 47–65.
- Maggi, C.A., and Meli, A. (1986). Suitability of urethane anesthesia for physiopharmacological investigations in various systems. Part 1: General considerations. *Experientia* 42, 109–114.
- Mosconi, T.M., Rice, F.L., and Song, M.J. (1993). Sensory innervation in the inner conical body of the vibrissal follicle-sinus complex of the rat. *J. Comp. Neurol.* 328, 222–251.
- Nicolelis, M.A.L., Baccala, L.A., Lin, R.C.S., and Chapin, J.K. (1995). Sensorimotor encoding by synchronous neural ensemble activity at multiple levels of the somatosensory system. *Science* 268, 1353–1358.
- O'Connor, S.M., Berg, R.W., and Kleinfeld, D. (2002). Coherent electrical activity between vibrissa sensory areas of cerebellum and neocortex is enhanced during free whisking. *J. Neurophysiol.* 87, 2137–2148.
- Pali, J., Rencz, B., and Hamori, J. (2000). Innervation of a single vibrissa in the whisker-pad of rats. *Neuroreport* 11, 849–851.
- Prigg, T., Goldreich, D., Carvell, G.E., and Simons, D.J. (2002). Texture discrimination and unit recordings in the rat whisker/barrel system. *Physiol. Behav.* 77, 671–675.
- Rice, F.L., Mance, A., and Munger, B.L. (1986). A comparative light microscopic analysis of the sensory innervation of the mystacial pad. I. Innervation of vibrissal follicle-sinus complexes. *J. Comp. Neurol.* 252, 154–174.
- Rice, F.L., Kinnman, E., Aldskogius, H., Johansson, O., and Arvidsson, J. (1993). The innervation of the mystacial pad of the rat as revealed by Pgp 9.5 immunofluorescence. *J. Comp. Neurol.* 337, 366–385.
- Semba, K., and Egger, M.D. (1986). The facial “motor” nerve of the rat: control of vibrissal movement and examination of motor and sensory components. *J. Comp. Neurol.* 247, 144–158.
- Shoykhet, M., Doherty, D., and Simons, D.J. (2000). Coding of deflection velocity and amplitude by whisker primary afferent neurons: implications for higher level processing. *Somatosens. Mot. Res.* 17, 171–180.
- Sosnik, R., Haidarliu, S., and Ahissar, E. (2001). Temporal frequency of whisker movement. I. Representations in brain stem and thalamus. *J. Neurophysiol.* 86, 339–353.
- Tracey, D.J., and Waite, P.M.E. (1995). Somatosensory system. In *The Rat Nervous System*, G. Paxinos, ed. (San Diego: Academic Press), pp. 689–704.
- Waite, P.M.E., and Jacquin, M.F. (1992). Dual innervation of the rat vibrissa: responses of trigeminal ganglion cells projecting through deep or superficial nerves. *J. Comp. Neurol.* 322, 233–245.
- Welker, W.I. (1964). Analysis of sniffing of the albino rat. *Behaviour* 22, 223–244.
- Zucker, E., and Welker, W.I. (1969). Coding of somatic sensory input by vibrissae neurons in the rat's trigeminal ganglion. *Brain Res.* 12, 138–156.